Table 2. Summary of W49 observations.

Frequency (Mhz)	Number of 10-minute integrations: On source	Off source	Detection limit: Flux (mks)*	Antenna temperature (°K)
111.22	5	3	60	260
111.54	1	1	50	210

* One flux unit (mks) equals 10^{-26} watt m^{-2} hz^{-1}.

used during the two observing periods: in July 1967 the off-source measurements were made with a declination offset of 2°, and in June 1968, with a right ascension offset of 3°. (The half-power beamwidth was 51 minutes of arc.) The radio source W49 lies on the ridge of galactic background emission such that the difference in the antenna temperature between on and off source was 800°K in both cases.

Mezger *et al.* (7) have measured the combined flux of the two components, thermal and nonthermal, that constitute W49. Their data show the 111-Mhz flux to be 60 flux units (mks), due almost entirely to the nonthermal source. Thus W49 contributes about 260°K to the on-off difference in antenna temperature; the remaining 540°K is due to the galactic background (Table 2). The upper limits for detectable emission- or absorption-line intensities were set by unforeseen instabilities in the 100-channel filter bank. These limits were based on the assumption that a valid signal would appear in two or more contiguous channels; therefore the limits apply to linewidths greater than 100 hz. On this assumption, we found no signals in our data that exceeded the detection limit of Table 2. If features were confined to a single channel and if this filter channel happened to be one of the ten that show instabilities from time to time, then detection would have been much more difficult.

In view of the estimated magnitudes of SH-line intensities, it is perhaps not surprising that we have thus far failed to detect the line. However, we are optimistic about the possibilities for detection once the transition frequencies have been measured to greater precision. This would make it feasible to improve the sensitivity by a factor of 50 and extend the search to many more sources.

M. L. MEEKS
M. A. GORDON
M. M. LITVAK
Lincoln Laboratory, Massachusetts Institute of Technology, Lexington

References and Notes

1. H. E. Radford and M. Linzer, *Phys. Rev. Lett.* **10**, 443 (1963).
2. H. E. Radford, personal communication.
3. M. M. Litvak, A. L. McWhorter, M. L. Meeks, H. J. Zeiger, *Astron. J.* **72**, 812 (1967).
4. ———, *Phys. Rev. Lett.* **17**, 821 (1966).
5. A. H. Barrett, *IEEE (Inst. Elec. Electron. Eng.) Trans. Mil. Electron.* **MIL-8**, 156 (1964).
6. L. H. Aller, *Handbuch der Physik* (Springer-Verlag, Berlin, 1958), vol. 51, p. 343.
7. P. G. Mezger, J. Schraml, Y. Terzian, *Astrophys. J.* **150**, 807 (1967).
8. We acknowledge helpful discussions with Drs. F. C. Drake and G. H. Pettengill. We thank Dr. H. E. Radford for providing revised values for the transition frequencies, and we thank the staff of the Arecibo Ionospheric Observatory for their assistance during observing and data processing. The Arecibo Ionospheric Observatory is operated by Cornell University with the support of the Advanced Research Projects Agency. Lincoln Laboratory is operated with support from the U.S. Air Force.

4 December 1968

Nitrogen Abundances in Chondritic Meteorites

Abstract. *Carrier-gas fusion extractions of total nitrogen in 22 chondritic meteorites indicate a wide variation in total nitrogen contents, ranging from 660 parts per million for an enstatite chondrite to 18 parts per million for an ordinary chondrite. Total nitrogen and total carbon contents of individual chondrites do not show a positive correlation.*

The abundances of nitrogen have been determined in 22 chondritic meteorites by a carrier-gas fusion extraction technique with a LECO Nitrox-6 nitrogen analyzer. Powdered samples (50 to 200 mg) were burned in a graphite crucible in an inert atmosphere (helium) with a LECO induction furnace. The powdered samples in capsules made of nitrogen-free tin were kept in a vacuum for 48 hours, and sealed under helium in a dry box. The combustion products (all nitrogen-containing compounds and dissolved nitrogen having been converted to molecular nitrogen) were passed over a catalyst, consisting of rare earth and copper oxide, at 400°C to convert any carbon monoxide present to carbon dioxide. A trap containing ascarite and anhydrone in the flow system removed the carbon dioxide and water and allowed other combustion products to pass on through. This procedure was necessary to allow resolution of the nitrogen peak on the chromatogram, otherwise the excess carbon monoxide produced from oxygen in the chondrites would have overlapped the nitrogen peak. The remaining combustion products were collected in a molecular-sieve trap at liquid-nitrogen temperature. After the collection period, the trap was warmed, and the condensed gases were flushed into a gas chromatograph molecular-sieve column. As the gases were eluted from the column, they were detected in sequence as they passed over a thermal conductivity cell in the chromatograph. Nitrogen counts from an integrator were plotted against standard samples to obtain a calibration curve.

Studies of artificially prepared standards containing nitrogen as nitrides, ammoniacal ions, and nitrates, as well as standard NBS steels (National Bureau of Standards), with nitrides and dissolved nitrogen, indicated that complete extraction and detection was achieved for each sample. Eleven analyses of different NBS steels ranging in nitrogen content from 6.3 to 165 ppm gave an average percentage difference from the certified values of only 1.4 percent. Background values that were subtracted from individual analyses had a maximum of 5 ppm nitrogen. This background included atmospheric contamination and a combustion crucible blank.

The data obtained for the abundances of nitrogen in enstatite, olivine-bronzite (H), olivine-hypersthene (L) and (LL), and carbonaceous chondrites are given in Table 1. Replicate analyses on the same powdered meteorite sample provide an index of the reproducibility of the meteorite sample taken.

The problem of whether the trace nitrogen contents are inherent in the chondrites or whether the nitrogen has been added during the terrestrial life of the meteorite has been studied by a heating experiment. A powdered sample of the Richardton chondrite was heated at 110°C for 48 hours. An analysis of the heat-treated sample gave nitrogen values of 47 and 61 ppm compared to values of 48 and 58 ppm for the untreated sample. We interpret this to indicate that the nitrogen in chondrites recovered immediately after falling is firmly bound and not a loosely adsorbed contamination product.

Previous determinations of nitrogen in chondrites have been largely limited

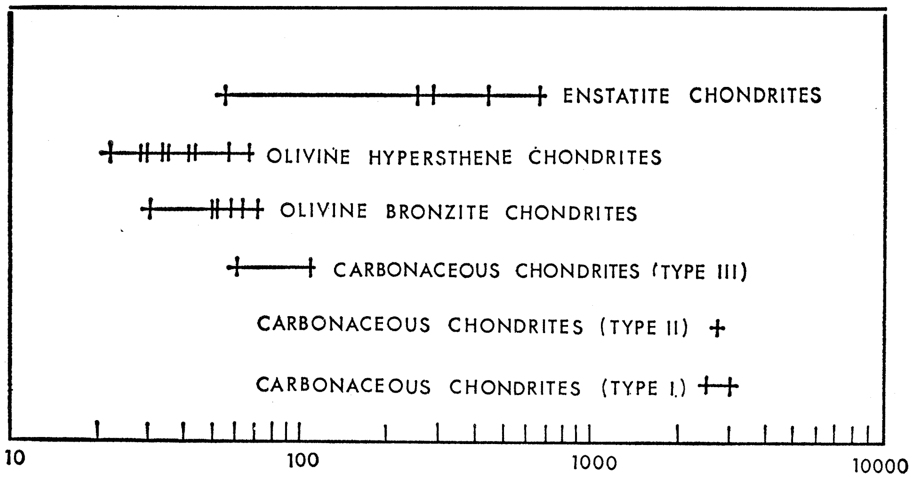

Fig. 1. Nitrogen abundances in chondrites (in parts per million).

to carbonaceous chondrites. Measurements of ordinary chondrites include those of Lipman (*1*) who reported combined nitrogen values ranging from 16 to 65 ppm in six meteorites, as determined by the Kjeldahl technique. Buddhue (*2*) reported that micro-Kjeldahl ammoniacal nitrogen in five chondrites ranged from 6 to 33 ppm. König *et al.* (*3*) determined ammoniacal nitrogen of six chondrites, and found that the mean was 7.8 ppm. Vinogradov *et al.* (*4*) reported that the ammoniacal nitrogen content determined by a chemical decomposition technique of four chondrites ranged from 8 to 38 ppm. Lipman's value for Forest City was 52 ppm as compared to our average value of 48 ppm and König's value was 10 ppm for New Concord as compared to ours of 21 ppm.

As indicated by the data of Table 1 and by Fig. 1, in which our values for nitrogen abundances and abundances for carbonaceous chondrites reported by Wiik (*5*) are plotted, individual meteorites within a given classification generally show a broad range of values. This type of distribution makes a calculated mean for a meteorite group of questionable value for comparison purposes.

Nitrogen and carbon abundances in individual chondrites do not show a positive correlation. It is of particular interest to note the relatively low nitrogen contents of the chondrites, Karoonda C4, Chainpur LL3, and Mokoia C3, compared to their relatively high carbon contents as reported in Moore and Lewis (*6*). The Hvittis enstatite chondrite, the only chondrite we used in which sinoite (Si_2N_2O) has been observed, contained the greatest total nitrogen content. Ordinary chondrites do not show a readily apparent relation between petrologic type and nitrogen content, although this is difficult to confirm on the basis of the limited data given.

The range of the analyses for nitrogen in the ordinary chondrites is from 18 to 75 ppm or, on the basis of 10^6 silicon atoms, from 99 to 396 nitrogen atoms. The nitrogen abundances reported here are considerably below the 800 nitrogen atoms per 10^6 silicon atoms in ordinary chondrites selected in the review by Larimer and Anders (*7*), who also noted that the three olivine-bronzite (H5) chondrites Allegan, Beardsley, and Richardton usually have increasing abundances of the volatile elements. While the total nitrogen content of Allegan is among the lowest of the chondrites measured, the contents for Beardsley and Richardton are similar and considerably higher, thus breaking the observed trend. Further work on the chemical state of nitrogen in chondrites may indeed indicate such a relationship between ammoniacal nitrogen and other volatile elements.

The distributions of nitrogen and carbon in the different chondrite groups are similar in most respects. Both elements show relatively higher abundances in the carbonaceous chondrites and the enstatite chondrites than in the ordinary chondrites. The only apparent variation in the distribution is in the type III carbonaceous chondrites in which nitrogen-bearing compounds have either not been accumulated or preserved to the same extent that those of carbon have been.

Table 1. Abundances of total nitrogen in chondrites.

Meteorite	Petrologic type (*8*)	Abundance (ppm)
	Enstatite chondrites	
Hvittis (contains Sinoite)	E6	660; 650; 600
Khairpur	E6	60; 40; 59
Abee	E4	295; 260; 264
Indarch	E4	431; 430; 448; 413
Atlanta	E5	275; 224; 260; 228
	Carbonaceous chondrites	
Karoonda	C4	67; 60; 48
Mokoia	C3	85; 125; 100
	Olivine-bronzite chondrites	
Forest City	H5	75; 30; 46; 42
Allegan	H5	25; 35
Richardton	H5	48; 58
Saline	H5	50; 47; 53
Kesen	H4	68; 40; 58
Beardsley	H5	60; 69; 49
	Olivine-hypersthene chondrites	
Bruderheim	L6	43; 28; 29; 28
New Concord	L6	18; 24
Leedey	L6	32; 35
Dhurmsala	LL6	42; 40; 42
Marion (Iowa)	L6	24; 34; 26
Farmington	L5	26; 31; 27
Ergheo	L5	73; 56; 65
Modoc	L6	36; 52; 32
Chainpur	LL6	57; 54; 55

CARLETON B. MOORE
EVERETT K. GIBSON
Center for Meteorite Studies, Arizona State University, Tempe 85281

References and Notes

1. C. B. Lipman, *Amer. Mus. Novitates* **589**, 2 (1932).
2. J. D. Buddhue, *Pop. Astron.* **50**, 560 (1942).
3. V. H. König, K. Keil, H. Hintenberger, F. Wlotzka, F. Begemann, *Z. Naturforsch.* **16a**, 1124 (1961).
4. A. P. Vinogradov, K. P. Florenskii, V. F. Volynets, *Geochemistry (USSR) (English Transl.)* **10**, 905 (1963).
5. H. B. Wiik (unpublished results) reported in B. Mason, *Meteorites* (Wiley, New York, 1962), p. 156.
6. C. B. Moore and C. F. Lewis, *Science* **149**, 317 (1965).
7. J. W. Larimer and E. Anders, *Geochim. Cosmochim. Acta* **31**, 1239 (1967).
8. W. R. Van Schmus and J. A. Wood, *ibid.*, p. 747. We thank C. F. Lewis for preparing the samples for analyses. All of the specimens used in this work are from the Center for Meteorite Studies collection at Arizona State University. Supported by NSF grant GA-909. Contribution No. 33 from Center for Meteorite Studies.

6 August 1968; revised 4 November 1968

Gravitational Mechanism for Sea-Floor Spreading

Abstract. *The gravitational attraction of the continents produces a force field at the surface of the earth, similar in geometry to lithospheric displacements deduced from studies of earthquake focal mechanisms.*

Proponents of a mobile, competent lithosphere comprising the surface of the solid earth (*1*, *2*) interpret most of the Cenozoic tectonism of the earth as the relative movements of, and interactions between, large plates of lithosphere, with much of the dynamic activity concentrated along the periphery of the plates. The geographical distribution of earthquakes and studies of their focal mechanisms provide perhaps the most detailed picture of these peripheral interactions as thought to be occurring. A summary of tectonic displacements as deduced from focal mechanism studies (*2*) is shown in Fig. 1. Only reliably determined slip vectors are depicted; tectonic displacements no doubt occur elsewhere, but remain undetermined.

Although the assemblage of many geological and geophysical observations points to the existence of a mobile lithosphere, the dynamical cause of the mobility is less clearly defined. Here I reexamine a mechanism, intrinsically simple, which may explain much of the motion of the oceanic lithosphere and its interaction with continental blocks. Directly stated, the continental masses produce a mutual attraction for each other and for the oceanic lithosphere. Jeffreys (*3*) estimated the magnitude of such attraction, but in his computations considered the continental topography to be fully compensated by its subsurface projection. The topography and its compensation taken together were characterized mathematically by a point doublet, the attractive field of which diminishes as the inverse third power of the distance from the doublet. Jeffreys obtained stresses on the order of 10^{-2} dyne/cm^2 acting on the lithospheric surface, a magnitude which he judged insufficient to move continents. The doublet remains in common usage as an isostatic correction in gravity studies.

In reexamining this gravitational mechanism, I postulate that the continental masses are to some degree uncompensated. The attraction of the uncompensated excess mass diminishes only as the inverse square of the distance from the mass, and thus presents the possibility of a stronger field than does the doublet. The distribution of excess mass can be represented by a surface density σ equal to a constant over the continents and zero over the oceans. This representation emphasizes only the fundamental contrast between continents and oceans, while ignoring regional variation within each. The gravitational potential of such a distribution of mass is given by $V = \int_A (G\sigma/r)\, dA$ where G is the universal gravitational constant and r is the distance between a mass element and the field point. The components of attraction can be obtained by forming the gradient of the potential. In this investigation the potential and attraction were obtained by direct numerical integration over a surface divided into segments bounded by successive 15° meridians and parallels.

The horizontal component of the computed attraction vector at the surface of the earth is shown in Fig. 2. This field represents the horizontal forces acting on the lithosphere according to the hypothesis of some uncompensated continental mass. The most prominent feature of this force field is the attraction of the continents for the ocean floor. All convergences of the vector field occur on the continents; all divergences occur in the oceans. At the continental margins the field is everywhere nearly perpendicular. A marked similarity between the slip vectors of Fig. 1 and the force vectors in corresponding localities is apparent. It is the shorter task to call attention to the principal area of disagreement, along the west coast of North America, where the vectors are a quadrant apart. Elsewhere the fields are sufficiently

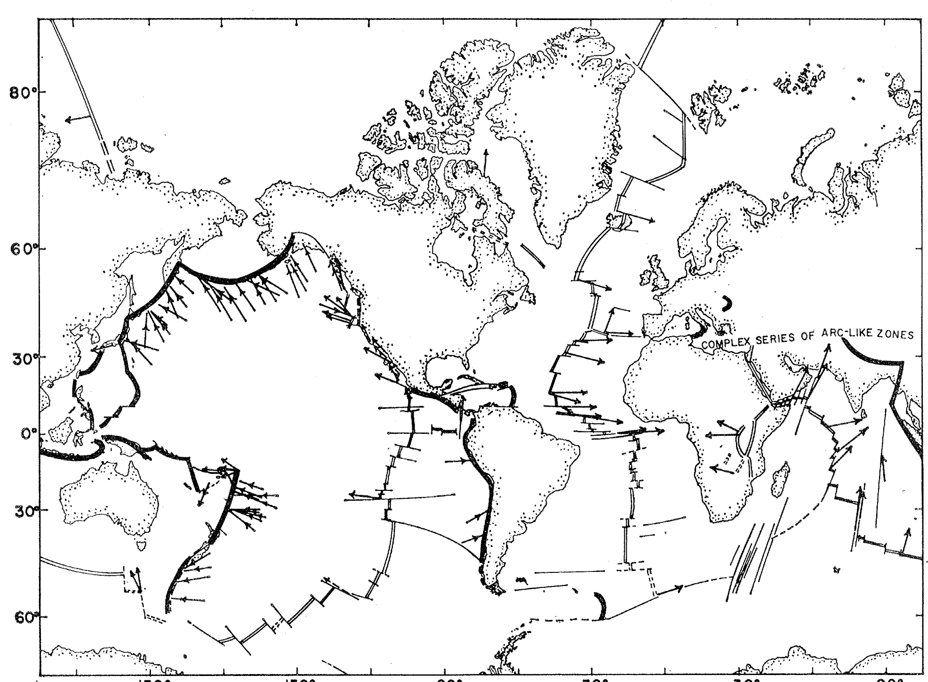

Fig. 1. Slip vectors derived from earthquake-mechanism studies. Symbols: arrows, horizontal component of direction of relative motion of block on which arrow is drawn to adjoining block; double lines, crests of world-rift system; bold single lines, islands arcs and arclike features; single lines, major transform faults [after Isacks and co-workers (*2*)].